Structure−Reactivity Relationships in Bimolecular-Activated Monomer Polymerization of (Meth)acrylates Using Oxidatively Activated Group 14 Ketene Acetals

Yuetao Zhang and Eugene Y.-X. Chen*

Department of Chemistry, Colorado State University, Fort Collins, Colorado 80523-1872

Received May 20, 2008; Revised Manuscript Received June 26, 2008

ABSTRACT: Highly active, bifunctional propagating species that contain both nucleophilic and electrophilic catalyst sites as well as bring about efficient living/controlled (meth)acrylate polymerization at ambient temperature via a bimolecular-activated monomer propagation mechanism have been generated by instantaneous oxidative activation of ketene silyl acetal initiators with a catalytic amount (0.05 mol % relative to monomer) of the trityl activator. Studies of structure−reactivity relationships for this novel polymerization system have included effects on the polymerization activity and the degree of control by structures of *initiator* (alkyl, silyl, germyl, and stannyl acetals), *catalyst* (variations in alkyl and silyl groups of the silyl acetals), *activator* (trityl salts of anions differing in their stability, size, coordination, and chirality), and *monomer* (methacrylates vs acrylates). Of several valuable findings obtained from this study, a most interesting and significant result is that there exhibits remarkable selectivity of the silyl group structure of the acetal initiator (and thus the derived silyl cation catalyst) for monomer structure: initiators having small silyl groups, such as dimethylketene methyl trimethylsilyl acetal, promote highly active and efficient polymerization of methacrylates, but they are poor initiators for polymerization of less sterically hindered, active α-H bearing acrylate monomers. On the other hand, initiators incorporating bulky silyl groups, such as the triisobutylsilyl derivative, exhibit low activity toward methacrylate polymerization but *exceptionally high activity* (completed reaction in 1 min), *efficiency* (achieved quantitative initiator efficiency), *and degree of control* (regulated low to high M_n ($> 10^5$) with narrow molecular weight distributions) for acrylate polymerization at ambient temperature in polar noncoordinating (CH_2Cl_2), aromatic (toluene), or aliphatic (cyclohexane) solvents.

Introduction

Anionic polymerization is a key technique to convert nonpolar and polar vinyl monomers in a living/controlled fashion to technologically important vinyl polymers with controlled structures.[1] In particular, anionic polymerization of polar vinyl monomers such as acrylic monomers at economically desirable conditions is challenging due to side reactions and the multiple-site nature of anionic active species derived from common organolithium reagents,[2] although many strategies have been developed to achieve various degrees of polymerization control.[3] Of these strategies is a particularly interesting and commercialized living/controlled polymerization process involving a silyl ketene acetal (SKA) initiator and a catalyst at ambient or higher polymerization temperatures. This polymerization was discovered by DuPont scientists and termed group transfer polymerization (GTP) based on the initially postulated *associative* propagation mechanism in which the silyl group coordinated with a nucleophilic catalyst is transferred intramolecularly to the incoming monomer through hypervalent anionic silicon species (path *a*, Scheme 1).[4] However, it has been recently concluded[5] that several lines of key experimental evidence now support a *dissociative* mechanism,[6] which involves ester enolate anions as propagating species and a rapid, reversible complexation (termination) of small concentrations of enolate anions with SKA or its polymer homologue (path *b*). Nevertheless, polymerization of methyl methacrylate (MMA) via GTP using a SKA and a nucleophilic catalyst such as a bifluoride or oxyanion (0.1−1.0 mol % relative to initiator)[7] can readily produce poly(methyl methacrylate) (PMMA) with number-average molecular weight (M_n) of ≤20 000 in a controlled fashion at $T \geq$ ambient temperatures, but its synthesis of PMMA with $M_n \geq 60\,000$ range is difficult.[5] Polymerization of *acrylates* using GTP requires use of Lewis acidic catalysts such as zinc halides or alkylaluminum chlorides and a much higher catalyst loading (typically 10 mol % based on monomer) to achieve a reasonable degree of polymerization control.[8]

Scheme 1. Associative and Dissociative Pathways for Group Transfer Polymerization (GTP) of Methyl Methacrylate (MMA) Using a Silyl Ketene Acetal (SKA) and a Nucleophilic (Nu) Catalyst

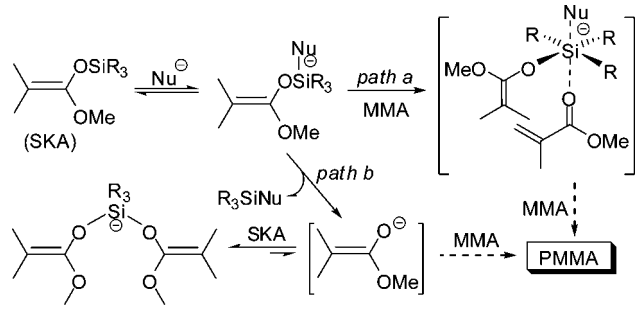

Activation of the inactive SKA is the critical first step in either the associative or dissociative pathway shown above, and it can be viewed that both paths *a* and *b* in GTP involve *reductive activation* of SKA. Direct oxidation of trialkylsilyl enol ethers of ketones by vinylogous hydride abstraction with trityl tetrafluoroborate, Ph_3CBF_4, led to formation of α,β-unsaturated ketones.[9] Hydride abstraction from an enolate methyl group of the zirconocene enolate complex $Cp_2ZrMe[OC(O^tBu){=}CMe_2]$ by trityl tetrakis(pentafluorophenyl)borate (TTPB), $Ph_3CB(C_6F_5)_4$,[10] gave a zirconocene−carboxylate dication, after subsequent elimination of methane and isobutene, serving as a catalyst deactivation pathway.[11] On the other hand, we found that *ansa*-zirconocene bis(ester enolate) complex $Me_2C(Cp)$-(fluorenyl)$Zr[OC(O^iPr){=}CMe_2]_2$ can be oxidatively activated with TTPB via vinylogous hydride abstraction from an enolate methyl group to give the isopropyl methacrylate coordinated

* Corresponding author. E-mail: eychen@lamar.colostate.edu.

10.1021/ma801125y CCC: $40.75
Published on Web 08/09/2008

Scheme 2. Initiation and Propagation Steps of the Bimolecular, Activated-Monomer Polymerization by $Me_2C{=}C(OMe)OSiMe_3$ (^{Me}SKA) Oxidatively Activated with $[Ph_3C][B(C_6F_5)_4]$ (Anion Omitted for Clarity)[19]

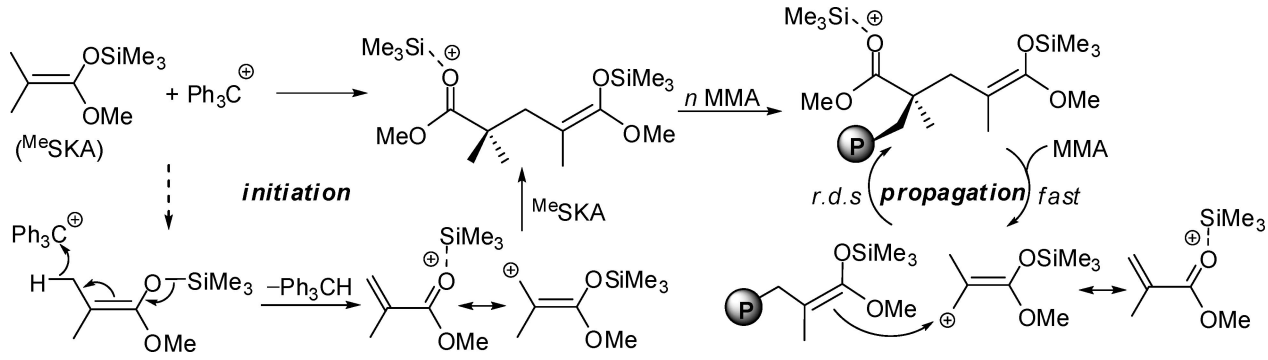

to Zr, and subsequent Michael addition of the other enolate ligand to this activated methacrylate monomer produced the cationic eight-membered-ring chelate, which is a highly active and stereoselective MMA polymerization catalyst.[12] TTPB is an important activator for metal-catalyzed olefin polymerization,[13] and it has also been used to successfully generate the highly reactive, solvated silyl cation (or silylium ion) "R_3Si^+", $[Et_3Si(toluene)]^+[B(C_6F_5)_4]^-$, from the reaction of Et_3SiH + TTPB in toluene via hydride abstraction.[14] Trityl salts in general are known to catalyze aldol condensations and Michael reactions involving nucleophiles such as silyl enol ethers or SKA and substrates such as acetals, aldehydes, or α,β-unsaturated ketones;[15] the trityl catalyst used in these reactions was proposed to activate the substrate via interaction between the trityl cation and alkoxy (or acyloxy) or carbonyl oxygen of the substrate.[15] Trimethylsilyl triflate also catalyzes aldol condensations of enol silyl ethers and acetals,[16] and its combination with bulky organoaluminum cocatalysts exhibits high activity toward the catalytic Mukaiyama aldol reaction of enol silyl ethers with aldehydes and ketones.[17] A combination of triethylsilyl triflate with $B(C_6F_5)_3$ has been found to promote GTP of acrylates initiated by SKA.[18]

We previously reported a novel living/controlled methacrylate polymerization using a combination of a SKA with a catalytic amount of the ubiquitous olefin polymerization activator TTPB.[19] An intriguing, "*monomer-less*" initiation step involves oxidative activation of dimethylketene methyl trimethylsilyl acetal (^{Me}SKA) by TTPB, leading to the Me_3Si^+-activated MMA (or silylated MMA) derived from vinylogous hydride abstraction of ^{Me}SKA with Ph_3C^+ (i.e., the monomer is generated from the initiator!); subsequent Michael addition of ^{Me}SKA to the activated MMA affords the highly active, bifunctional active species containing both nucleophilic SKA and electrophilic silyl cation catalyst sites (see the initiation manifold, Scheme 2). The use of the borane $B(C_6F_5)_3$ did not effect hydride abstraction of SKA. A propagation "catalysis" cycle in the MMA polymerization by the oxidatively activated SKA with TTPB consists of a fast step of recapturing the silyl cation catalyst from the ester group of the growing polymer chain by the incoming MMA, followed by a rate-determining step of the C−C bond formation via intermolecular Michael addition of the polymeric SKA to the silylated MMA (see the propagation manifold, Scheme 2; resonance forms of the isoelectronic adduct $MMA\cdot Al(C_6F_5)_3$ were previously described[2]). According to the polymerization kinetics and mechanism, this polymerization is characterized as a bimolecular-activated monomer polymerization, resembling that by the isoelectronic enolaluminate/alane pair[2,20] or the zirconocene enolate/zirconocenium pair.[21] It is also a living/controlled methacrylate polymerization, readily producing PMMA of low to high M_n ($>10^5$) with narrow molecular weight distributions (MWDs) (polydispersity index, PDI, = 1.04−1.12) at ambient temperature, with a trityl catalyst loading as low as 0.025 mol % (based on monomer).

The central objective of the current study is to investigate structure−reactivity relationships for this new polymerization system. Accordingly, this study has focused on the following four subjects: (a) oxidative activation reactions of dimethylketene group 14 (alkyl, silyl, germyl, and stannyl) acetals with TTPB and effectiveness of the resulting products for (meth-)acrylate polymerization; (b) effects of alkyl and silyl groups of acetals; (c) effects of anion structure of trityl salt activators; and (d) effects of monomer structure (methacrylates vs acrylates). These initiator, activator, catalyst, and monomer structural effects have been carefully examined in terms of their influences on polymerization activity and control.

Experimental Section

Materials, Reagents, and Methods. All syntheses and manipulations of air- and moisture-sensitive materials were carried out in flamed Schlenk-type glassware on a dual-manifold Schlenk line, on a high-vacuum line, or in an argon-filled glovebox. NMR-scale reactions (typically in a 0.02 mmol scale) were conducted in Teflon-valve-sealed J. Young-type NMR tubes. High-performance liquid chromatography (HPLC) grade organic solvents were first sparged extensively with nitrogen during filling 20 L solvent reservoirs and then dried by passage through activated alumina [for diethyl ether (Et_2O), tetrahydrofuran (THF), and CH_2Cl_2] followed by passage through Q-5-supported copper catalyst (for toluene and hexanes) stainless steel columns. Benzene-d_6 and toluene-d_8 were dried over sodium/potassium alloy and vacuum-distilled or filtered, whereas C_6D_5Br, CD_2Cl_2, and $CDCl_3$ were dried over activated Davison 4 Å molecular sieves. NMR spectra were recorded on either a Varian Inova 300 (FT 300 MHz, ^{1}H; 75 MHz, ^{13}C; 282 MHz, ^{19}F) or a Varian Inova 400 spectrometer. Chemical shifts for ^{1}H and ^{13}C spectra were referenced to internal solvent resonances and are reported as parts per million relative to $SiMe_4$, whereas ^{19}F NMR spectra were referenced to external $CFCl_3$. High-resolution mass spectrometry (HRMS) data were collected using Agilent 6220 accurate time-of-flight LC/MS spectrometer.

MMA (99%) and *n*-butyl methacrylate (BMA; 99%) were purchased from Aldrich Chemical Co., while *n*-butyl acrylate (*n*-BA) was purchased from Acros. The monomers were first degassed and dried over CaH_2 overnight, followed by vacuum distillation, and final purification of MMA involved titration with neat tri(*n*-octyl)aluminum (Strem Chemicals) to a yellow end point[22] followed by vacuum distillation. The purified monomers were stored in brown bottles inside a −30 °C glovebox freezer. Butylated hydroxytoluene (BHT-H, 2,6-di-*tert*-butyl-4-methylphenol) was purchased from Aldrich Chemical Co. and recrystallized from hexanes prior to use. Tris(pentafluorophenyl)borane $B(C_6F_5)_3$ and trityl tetrakis(pentafluorophenyl)borate $[Ph_3C][B(C_6F_5)_4]$ were obtained as a research gift from Boulder Scientific Co.; $B(C_6F_5)_3$ was further purified by recrystallization from hexanes at −30 °C, whereas $[Ph_3C][B(C_6F_5)_4]$

was used as received. Tris(pentafluorophenyl)alane $Al(C_6F_5)_3$, as a 0.5 toluene adduct $Al(C_6F_5)_3 \cdot (C_7H_8)_{0.5}$, was prepared by the reaction of $B(C_6F_5)_3$ and $AlMe_3$ in a 1:3 toluene/hexanes solvent mixture in quantitative yield;[23] this is the modified synthesis based on literature procedures.[24] Although we have experienced no incidents when handling this material, *extra caution should be exercised*, especially when dealing with the unsolvated form, because of its thermal and shock sensitivity. Dimethylketene methyl trimethylsilyl acetal (^{Me}SKA, 95%), diisopropylamine (≥99%), methyl isobutyrate (99%), chlorotriisobutylsilane (99%), chlorotrimethylsilane (99%), isopropyl isobutyrate (99%), and benzyl chloride (99%) were purchased from Aldrich and dried over CaH_2, followed by vacuum distillation. PCl_5 (95%), Ph_3CCl (98%), Ph_3CBF_4 (≥97%), Bu_3N (98.5+%), NaH (95%), Ph_3SiCl (96%), Me_3GeCl (98%), and Me_3SnCl (97%) were purchased from Aldrich and used as received. Literature procedures were employed for the preparation of the following compounds: dimethylketene dimethyl acetal (DKDA) $Me_2C{=}C(OMe)_2$,[25] dimethylketene methyl triethylsilyl acetal (^{Et}SKA) $Me_2C{=}C(OMe)OSiEt_3$,[19] dimethylketene isopropyl trimethylsilyl acetal $Me_2C{=}C(O^iPr)OSiMe_3$,[26] $[Ph_3C][(C_6F_5)_3Al{-}F{-}Al(C_6F_5)_3]$,[27] and trityl [tris(tetrachlorobenzenediolato) phosphate(V)] $[Ph_3C][$*rac*-TRISPHAT$]$.[28]

Dimethylketene Methyl Triphenylsilyl Acetal $Me_2C{=}C(OMe)OSiPh_3$ (^{Ph}SKA).[29] Literature procedures for the general synthesis of ketene trialkylsilyl acetals[30] were modified to prepare ^{Ph}SKA. In an argon-filled glovebox, a 200 mL Schlenk flask was equipped with a stir bar and charged with THF (100 mL) and diisopropylamine (5.00 mL, 3.61 g, 35.7 mmol). This flask was sealed with a rubber septum, removed from the glovebox, interfaced to a Schlenk line, and placed in a 0 °C ice−water bath. *n*-Butyllithium (23.4 mL, 1.6 M in hexane, 37.5 mmol) was added dropwise via syringe to the above flask. After being stirred at 0 °C for 30 min, methyl isobutyrate (4.09 mL, 3.64 g, 35.7 mmol) was added to this solution. The resulting mixture was stirred at this temperature for 30 min, after which chlorotriphenylsilane (10.8 g, 36.6 mmol) was added. The mixture was allowed to warm slowly to room temperature and stirred for 3 h at this temperature, after which all volatiles were removed in vacuum and hexanes (50 mL) was added. The resulting precipitates were filtered off under argon atmosphere; the filtrate was cooled to −30 °C inside a freezer of the glovebox overnight, affording ^{Ph}SKA as colorless crystals. The combined yield from several crops of recrystallization, after filtration and drying, was 8.67 g (67.4%). ^{1}H NMR ($CDCl_3$, 300 MHz, 23 °C): δ 7.71−7.68 (m, 6H, *o*-H of *Ph*), 7.47−7.38 (m, 9H, *m,p*-H of *Ph*), 3.21 (s, 3H, O*Me*), 1.58 (s, 3H, =C*Me*), 1.59 (s, 3H, =C*Me*). ^{13}C NMR ($CDCl_3$, 75 MHz, 23 °C): δ 150.2 [=*C*(OMe)], 135.8, 134.1, 130.4, 128.0 (Ph), 92.59 (=*C*Me$_2$), 58.44 (O*Me*), 17.33, 16.44 (=C*Me*).

Dimethylketene Methyl Triisobutylsilyl Acetal $Me_2C{=}C(OMe)OSi(^iBu)_3$ (^{iBu}SKA). The title compound was prepared using chlorotriisobutylsilane (5.0 g, 21.3 mmol) in the same manner as for the synthesis of ^{Ph}SKA, except that vacuum distillation was used to give the final product (5.30 g, 82.8% yield) as a colorless oil. ^{1}H NMR (C_6D_6, 400 MHz, 23 °C): δ 3.38 (s, 3H, O*Me*), 1.98 (sept, J = 6.8 Hz, 3H, C*H*Me$_2$), 1.71 (s, 3H, =C*Me*), 1.70 (s, 3H, =C*Me*), 1.05 (d, J = 6.8 Hz, 18H, CH*Me*$_2$), 0.84 (d, J = 6.8 Hz, 6H, C*H*$_2$CHMe$_2$). ^{13}C NMR (C_6D_6, 100 MHz, 23 °C): δ 151.7 [=*C*(OMe)], 91.24 (=*C*Me$_2$), 58.03 (O*Me*), 27.08 (CH*Me*$_2$), 26.76 (*C*HMe$_2$), 24.87 (*C*H$_2$CHMe$_2$), 17.77, 16.93 (=C*Me*). HRMS (APCI) *m/z* calcd for $C_{17}H_{36}O_2Si$ $[M + H]^+$: 301.2557; found: 301.2557.

Dimethylketene Methyl Tris(trimethylsilyl)silyl Acetal $Me_2C{=}C(OMe)OSi(SiMe_3)_3$ (^{TMS}SKA). The title compound was prepared using chlorotris(trimethylsilyl)silane (5.0 g, 17.7 mmol) in the same manner as for the synthesis of ^{Ph}SKA, except that vacuum distillation was used to give the final product (1.7 g, 28% yield) as a colorless oil. ^{1}H NMR (C_6D_6, 400 MHz, 23 °C): δ 3.30 (s, 3H, O*Me*), 1.68 (s, 3H, =C*Me*), 1.62 (s, 3H, =C*Me*), 0.31 (s, 27H, Si*Me*$_3$). ^{13}C NMR (C_6D_6, 100 MHz, 23 °C): δ 153.52 [=*C*(OMe)], 91.58 (=*C*Me$_2$), 58.31 (O*Me*), 17.95, 16.86 (=C*Me*), 0.76 (Si*Me*$_3$).

Methyl 2-(Trimethylgermyl)isobutyrate $Me_2C(GeMe_3)C(OMe){=}O$.[7] The title compound was obtained using chlorotrimethylgermane (5.0 g, 32.6 mmol) instead of chlorotriphenylsilane in the same manner as for the synthesis of ^{Ph}SKA, except that vacuum distillation was used to give the final product (4.70 g, 65.8% yield) as a colorless oil. ^{1}H NMR ($CDCl_3$, 300 MHz, 23 °C): δ 3.63 (s, 3H, O*Me*), 1.25 (s, 6H, C*Me*$_2$), 0.16 (s, 9H, Ge*Me*$_3$). ^{13}C NMR ($CDCl_3$, 75 MHz, 23 °C): δ 178.9 (*C*=O), 51.40 (O*Me*), 33.80 (*C*Me$_2$), 20.91 (C*Me*$_2$), −4.16 (Ge*Me*$_3$). HRMS (APCI) *m/z* calcd for $C_8H_{18}O_2[^{74}Ge]$ $[M + H]^+$: 221.0597; found: 221.0595.

Methyl 2-(Trimethylstannyl)isobutyrate $Me_2C(SnMe_3)C(OMe){=}O$.[7] The title compound was obtained using chlorotrimethylstanne (4.0 g, 20.1 mmol) instead of chlorotriphenylsilane in the same manner as for the synthesis of ^{Ph}SKA, except that vacuum distillation at 23−24 °C (0.3 Torr) was used to give the final product (1.70 g, 32.0% yield) as a colorless oil. ^{1}H NMR ($CDCl_3$, 300 MHz, 23 °C): δ 3.57 (s, 3H, O*Me*), 1.33 (s, 2d, J_{119Sn} = 54 Hz, J_{117Sn} = 50 Hz, 6H, C*Me*$_2$), 0.08 (s, 2d, J_{119Sn} = 51.6 Hz, J_{117Sn} = 50 Hz, 9H, Sn*Me*$_3$). ^{13}C NMR ($CDCl_3$, 75 MHz, 23 °C): δ 179.3 (*C* = O), 51.19 (O*Me*), 32.42 (*C*Me$_2$), 22.08 (C*Me*$_2$), −10.37 (s, 2d, J_{119Sn} = 325 Hz, J_{117Sn} = 311 Hz, Sn*Me*$_3$). HRMS (EI+) *m/z* calcd for $C_8H_{18}O_2[^{120}Sn]$ $[M]^+$: 266.0329; found: 266.0327.

Methyl 2,2-Dimethyl-3-Phenyl Propanoate $PhCH_2CMe_2C(OMe){=}O$.[31] The title compound was obtained using benzyl chloride (5.0 g, 39.5 mmol) instead of chlorotriphenylsilane in the same manner as for the synthesis of ^{Ph}SKA, except that vacuum distillation was used to give the final product (6.70 g, 88.2% yield) as a colorless oil. ^{1}H NMR ($CDCl_3$, 300 MHz, 23 °C): δ 7.32−7.23 (m, 3H, *m,p*-H of *Ph*), 7.14−7.12 (d, 2H, *o*-H of *Ph*), 3.68 (s, 3H, O*Me*), 2.88 (s, 2H, *CH*$_2$Ph), 1.21 (s, 6H, C*Me*$_2$). ^{13}C NMR ($CDCl_3$, 75 MHz, 23 °C): δ 178.1 (*C*=O), 138.0, 130.3, 128.2, 126.6 (Ph), 51.84 (O*Me*), 46.55 (*C*H$_2$Ph), 43.83 (*C*Me$_2$), 25.11 (C*Me*$_2$). HRMS (APCI) *m/z* calcd for $C_{12}H_{16}O_2$ $[M + H]^+$: 193.1223; found: 193.1224.

Reaction of $Me_2C{=}C(OMe)_2$ with $[Ph_3C][B(C_6F_5)_4]$ for Generation of $[(MeO)_2C{=}CMeCH_2CMe_2C(OMe)_2]^+[B(C_6F_5)_4]^-$ (1). In an argon-filled glovebox, a Teflon-valve-sealed J. Young-type NMR tube was charged with DKDA (4.60 mg, 0.04 mmol) and 0.3 mL of CD_2Cl_2. A CD_2Cl_2 (0.3 mL) solution of TTPB (18.5 mg, 0.02 mmol) was slowly added to this tube via pipet at ambient temperature. The mixture was allowed to react for ∼15 min before NMR spectra were recorded, which showed the clean formation of ion pair **1** and coproduct Ph_3CH. ^{1}H NMR (CD_2Cl_2, 300 MHz, 23 °C) for Ph_3CH: δ 7.31−7.21 (m, 9H, *m,p*-H of *Ph*), 7.13 (d, 6H, *o*-H of *Ph*), 5.55 (s, 1H, C*H*). ^{1}H NMR (CD_2Cl_2, 300 MHz, 23 °C) for **1**: δ 4.58 [s, 6H, C(O*Me*)$_2^+$], 3.55 (s, 3H, =CO*Me*), 3.51 (s, 3H, =CO*Me*), 2.48 (s, 2H, =CC*H*$_2$), 1.66 (s, 3H, =C*Me*), 1.49 (s, 6H, C*Me*$_2$). ^{19}F NMR (CD_2Cl_2, 282 MHz, 23 °C): δ −131.5 (s, br. 8F, *o*-F of C_6F_5), −161.9 (t, J = 20.3 Hz, 4F, *p*-F of C_6F_5), −165.8 (m, 8F, *m*-F of C_6F_5).

The colorless single crystals of **1** were obtained by layering a hexane solution of 2 equiv of DKDA onto a CH_2Cl_2 solution of TTPB at −30 °C inside a freezer of the glovebox for 1 week. The ^{1}H NMR of the isolated crystals is identical to that of **1**, generated in situ in NMR-scale reactions. The molecular structure of **1** was characterized by single-crystal X-ray diffraction analysis (vide infra).

Reaction of $Me_2C(GeMe_3)C(OMe){=}O$ with $[Ph_3C][B(C_6F_5)_4]$. In an argon-filled glovebox, a Teflon-valve-sealed J. Young-type NMR tube was charged with 8.8 mg (0.04 mmol) of $Me_2C(GeMe_3)C(OMe){=}O$ and 0.3 mL of CD_2Cl_2. A 0.3 mL CD_2Cl_2 solution of TTPB (18.5 mg, 0.02 mmol) was slowly added to this tube via pipet at room temperature. The mixture was allowed to react for ∼15 min at room temperature before the NMR spectra were recorded. Little reaction took place at this temperature up to 5 h, giving a mixture containing predominately the unreacted starting materials, plus a small amount of Ph_3CH, $[Ph_2C{=}C(CH{=}CH)_2CHCMe_2C(OMe){=}O{\cdots}GeMe_3][B(C_6F_5)_4]$ (**A**),[19] and $[MMA{\cdots}GeMe_3][B(C_6F_5)_4]$ (**B**). Subsequently, the reaction mixture was kept at 80 °C overnight. Species **A** disap-

peared, and species **B**, Ph_3CH, and $[Me_2CHC(OMe)=O\cdots GeMe_3][B(C_6F_5)_4]$ (**C**), plus the starting materials, were found present in the mixture.

^1H NMR (CD_2Cl_2, 300 MHz, 25 °C) for **A**: δ 7.31−7.14 (m, 10H, *Ph*), 6.54 (d, J = 10.5 Hz, 2H, C(C*H*=CH)$_2$CH), 5.72 (dd, J = 10.5 and 4.2 Hz, 2H, C(CH=C*H*)$_2$CH), 3.73 (s, 3H, O*Me*), 3.50 (t, J = 4.2 Hz, 1H, C(CH=CH)$_2$C*H*), 1.17 (s, 6H, C*Me*$_2$), 1.05 (s, 9H, Ge*Me*$_3$). **B**: δ 6.09 (br. s, 1H, =C*H*), 5.68 (br s, 1H, =C*H*), 3.80 (s, 3H, O*Me*), 1.95 (s, 3H, =C*Me*), 0.95 (s, 9H, Ge*Me*$_3$). **C**: δ 3.73 (s, 3H, O*Me*), 2.69 (sept, J = 6.9 Hz, 1H, C*H*Me$_2$), 1.28 (d, J = 6.9 Hz, 6H, CH*Me*$_2$), 1.17 (s, 9H, Ge*Me*$_3$). ^{19}F NMR (CD_2Cl_2, 282 MHz, 25 °C) for the $[B(C_6F_5)_4]$ anion: δ −131.4 (s, br, 8F, *o*-F of C_6F_5), −162.0 (t, J = 20.3 Hz, 4F, *p*-F of C_6F_5), −165.8 (m, 8F, *m*-F of C_6F_5).

Reaction of $Me_2C(SnMe_3)C(OMe)=O$ with $[Ph_3C][B(C_6F_5)_4]$. In an argon-filled glovebox, a Teflon-valve-sealed J. Young-type NMR tube was charged with 10.6 mg (0.04 mmol) of $Me_2C(SnMe_3)C(OMe)=O$ and 0.3 mL of CD_2Cl_2. A 0.3 mL CD_2Cl_2 solution of TTPB (18.5 mg, 0.02 mmol) was slowly added to this tube via pipet at room temperature. The mixture was allowed to react for ∼15 min at room temperature before the NMR spectra were recorded. The species $[Ph_2C=C(CH=CH)_2CHCMe_2C(OMe)=O\cdots SnMe_3][B(C_6F_5)_4]$ (**D**) (analogous to **A**) was the major product, plus a small amount of $[MMA\cdots SnMe_3][B(C_6F_5)_4]$ (**E**) (analogous to **B**) and the unreacted starting materials. This reaction mixture was kept at room temperature for 5 h, and no further reaction took place. Subsequently, the mixture was heated at 80 °C overnight. Species **D** disappeared, and species **E**, Ph_3CH, and $[Me_2CHC(OMe)=O\cdots SnMe_3][B(C_6F_5)_4]$ (**F**) (analogous to **C**), plus the starting materials, were found present in the final mixture.

^1H NMR (CD_2Cl_2, 300 MHz, 25 °C) for **D**: δ 7.32−7.13 (m, 10H, *Ph*), 6.61 (d, J = 10.2 Hz, 2H, C(C*H*=CH)$_2$CH), 5.61 (dd, J = 10.5 and 4.2 Hz, 2H, C(CH=C*H*)$_2$CH), 3.79 (s, 3H, O*Me*), 3.50 (t, J = 4.2 Hz, 1H, C(CH=CH)$_2$C*H*), 1.21 (s, 6H, C*Me*$_2$), 0.97 (s, 9H, Sn*Me*$_3$). **E**: δ 6.15 (br s, 1H, =C*H*), 6.02 (br s, 1H, =C*H*), 3.97 (s, 3H, O*Me*), 1.99 (s, 3H, =C*Me*), 0.98 (s, 9H, Sn*Me*$_3$). **F**: δ 3.95 (s, 3H, O*Me*), 3.00 (sept, J = 6.6 Hz, 1H, C*H*Me$_2$), 1.07 (d, J = 6.6 Hz, 6H, CH*Me*$_2$), 0.84 (s, 9H, Sn*Me*$_3$). ^{19}F NMR (CD_2Cl_2, 282 MHz, 25 °C) for the $[B(C_6F_5)_4]$ anion: δ −131.5 (s, br, 8F, *o*-F of C_6F_5), −162.0 (t, J = 20.3 Hz, 4F, *p*-F of C_6F_5), −165.8 (m, 8F, *m*-F of C_6F_5).

General Polymerization Procedures. Polymerizations were performed either in 30 mL oven- dried glass reactors inside the glovebox or in 25 mL oven- and flame-dried Schlenk flasks interfaced to the dual-manifold Schlenk line. SKA initiator and monomer were premixed, and the polymerization was started by addition of the activator TTPB or $[Ph_3C][TRISHAT]$. After the measured time interval, the polymerization was quenched by addition of 5 mL of 5% HCl-acidified methanol. For MMA and BMA homo- and copolymerizations, the quenched mixture was precipitated into 100 mL of methanol, stirred for 1 h, filtered, washed with methanol, and dried in a vacuum oven at 50 °C overnight to a constant weight. For *n*-BA polymerization, the polymer was isolated by evaporation of solvent and dried in a vacuum oven at room temperature to a constant weight.

A Selected Real Polymerization Example. In a argon-filled glovebox, a 30 mL, oven-dried glass reactor was charged with TTPB (4.3 mg, 4.7 μmol) in 5 mL of toluene. In a 20 mL glass vial $^{i\text{Bu}}$SKA (15.5 mg, 51.6 μmol) and *n*-BA (1.34 mL, 9.35 mmol) were mixed in 5 mL of toluene. The mixture was rapidly poured into the reactor to start the polymerization at ambient temperature (∼25 °C). The [*n*-BA]:[$^{i\text{Bu}}$SKA]:[TTPB] ratio in this selected example is 400:2.2:0.2, and the [monomer (M)]/[initiator (I)] ratio is 200. (For a polymerization with an x[M]$_0$/y[SKA]$_0$/z[TTPB]$_0$ ratio, the *total* equivalency of the propagating SKA = $y - 2z + z = y - z$, giving a [M]/[I] ratio of $x/(y - z)$.[19]) The reaction was stirred at ambient temperature for 1 min, after which a 0.2 mL aliquot was withdrawn from the reaction mixture using syringe and quickly quenched into a 1 mL vial containing 0.6 mL of undried "wet" $CDCl_3$ mixed with 250 ppm of BHT-H. The reactor was taken out of the glovebox, and the reaction was quenched by addition of 5 mL of 5% HCl-acidified methanol. The quenched mixture was isolated by evaporation of solvent and dried in a vacuum oven at room temperature to a constant weight. The quenched aliquot was analyzed by ^1H NMR to give 100% monomer conversion. The isolated and dried polymer was analyzed by gel permeation chromatography (GPC) to give $M_n = 2.31 \times 10^4$ g/mol and PDI = 1.07, relative to the PMMA standards. The dried P(*n*-BA) was also analyzed by ^1H NMR ($CDCl_3$, 300 MHz, 23 °C): δ 4.03 (m, O*CH*$_2$), 2.27 (s, br, C*H*), 1.89 (s, br, C*H*$_2$), 1.59 (m, C*H*$_2$ + OCH$_2$*CH*$_2$CH$_2$CH$_3$), 1.37 (m, OCH$_2$CH$_2$*CH*$_2$CH$_3$), 0.93 (t, *CH*$_3$).

Polymerization Kinetics. Kinetic experiments were carried out in a stirred glass reactor at ambient temperature (∼25 °C) inside the glovebox using stock solutions of the reagents and the procedures described in the literature.[2,32]

Polymer Characterizations. Polymer number-average molecular weight (M_n) and polydispersity index (PDI = M_w/M_n) were measured by GPC analyses carried out at 40 °C and a flow rate of 1.0 mL/min, with $CHCl_3$ as the eluent on a Waters University 1500 GPC instrument equipped with one PLgel 5 μm guard and three PLgel 5 μm mixed-C columns (Polymer Laboratories; linear range of molecular weight = 200−2 000 000). The instrument was calibrated with 10 PMMA standards, and chromatograms were processed with Waters Empower software (version 2002). ^1H NMR spectra for the analysis of PMMA and PBMA microstructures were recorded in $CDCl_3$ and analyzed according to the literature.[33]

X-ray Crystallographic Analysis of $[(MeO)_2C=CMeCH_2CMe_2C(OMe)_2]^+[B(C_6F_5)_4]^-$ (1). Single crystals suitable for X-ray diffraction were quickly covered with a layer of Paratone-N oil (Exxon, dried and degassed at 120 °C/10^{-6} Torr for 24 h) after the mother liquor was decanted and then mounted on a thin glass fiber and transferred into the cold nitrogen stream of a Bruker SMART CCD diffractometer. The structures were solved by direct methods and refined using the Bruker SHELXTL program library by full-matrix least-squares on F^2 for all reflections.[34] All non-hydrogen atoms were located by difference Fourier synthesis and refined with anisotropic displacement parameters. All hydrogen atoms were included geometrically with U_{iso} tied to the U_{iso} of the parent atoms and refined isotropically. A hexanes solvent molecule was found in lattice, and the Platon Squeeze program was applied to take care of the solvent void in the structure refinement.

X-ray crystal structural data for complex **1**: $C_{36}H_{23}BF_{20}O_4$, M_r = 910.35, T = 100(2) K, λ = 0.710 73 Å, crystal dimensions 0.30 × 0.15 × 0.03 mm^3, tetragonal, *I*4(1)/*a*, a = 34.2576(6) Å, b = 34.2576(6) Å, c = 13.1525(5) Å, V = 15 435.6(7) Å^3, Z = 16, ρ_{calcd} = 1.567 Mg/m^3, θ range for data collection = 2.36°−30.99°, 167 383 reflections collected, 12 281 unique (R_{int} = 0.0681), goodness-of-fit on F^2 = 1.090, final R_1 = 0.0544 and wR_2 = 0.1221 with $I > 2\sigma(I)$, residual electron density extremes = 0.401 and −0.289 e Å^{-3}.

Results and Discussion

Reaction of Group 14 Dimethylketene Acetals with TTPB. Dimethylketene *silyl* acetals such as $^{\text{Me}}$SKA can be spontaneously oxidatively activated with TTPB at ambient temperature, generating highly active, bifunctional active species containing both nucleophilic SKA and electrophilic silyl cation catalyst sites.[19] To investigate whether other group 14-based ketene acetals could be activated in the same fashion to generate active propagating species or not, we extended our study of oxidative activation of ketene acetals to include carbon, germanium, and tin-based ketene acetals.

The dimethylketene dimethyl acetal (DKDA) is indeed readily activated with TTPB in the same fashion as the silyl acetal $^{\text{Me}}$SKA. Specifically, the 2:1 ratio reaction of DKDA with TTPB in CD_2Cl_2 at room temperature produces cleanly the anticipated C−C bond coupling product **1** according to the analysis of the NMR data (see Experimental Section), with concomitant formation of Ph_3CH. Formation of **1** can be explained by conjugate addition of DKDA to the Me^+-activated MMA (methylated MMA) generated by vinylogous *hydride abstraction* of DKDA

Scheme 3. Oxidative Activation of $Me_2C{=}C(OMe)_2$ by $[Ph_3C][B(C_6F_5)_4]$

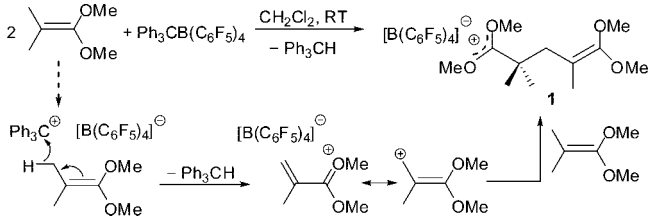

with Ph_3C^+ (Scheme 3), following the same pathway already established for the reaction of SKA and TTPB.[19]

The spectroscopically derived structure of **1** has been confirmed by single-crystal X-ray diffraction analysis (Figure 1), featuring the C−C bond coupling product containing both neutral ketene acetal and cationic acetal moieties. As anticipated, the sums of the angles around both ketene acetal C(27) and cationic C(34) carbons are 360.0° and 359.9°, respectively, for sp^2-hybridized, trigonal-planar carbon centers. However, as the structure of **1** shows, C(27) forms a double bond with a neighboring C(28) having a bond length of 1.325(3) Å, whereas C(34) forms a single bond with a neighboring C(31) exhibiting a bond length of 1.514(3) Å. Furthermore, the O−C bonds within the cationic acetal moiety are ∼0.1 Å shorter than those found in the neutral ketene acetal moiety in **1**. Overall, the positive charge on the cationic acetal carbon is delocalized onto the two neighboring oxygen atoms via $p_\pi-p_\pi$ interactions, characteristic of an oxocarbenium ion.

The structural characterization of this oxidatively activated product of the dimethylketene acetal also indirectly verified the analogous C−C bond coupling product structure derived from the oxidative activation of the silyl acetal analogue, which was not structurally characterized as single crystals suitable for X-ray diffraction analysis were not obtained.[19] On the other hand, unlike its silyl acetal analogue, the carbon-based structure **1** generated by oxidative activation of DKDA with TTPB is *inactive* toward polymerization of (meth)acrylates; however, it is active for the homopolymerization of DKDA, leading to the corresponding polyacetal (which is unstable toward air/moisture) via presumably a cationic polymerization pathway.

As the reaction of the in situ generated lithium enolate $Me_2C{=}C(OMe)OLi$ with $ClSiR_3$ has been proven to be general for the exclusive formation of O-bound trialkylsilyl, triarylsilyl, or trisilylsilyl ketene acetals (Scheme 4, see Experimental Section), by employing the same route, we attempted synthesis

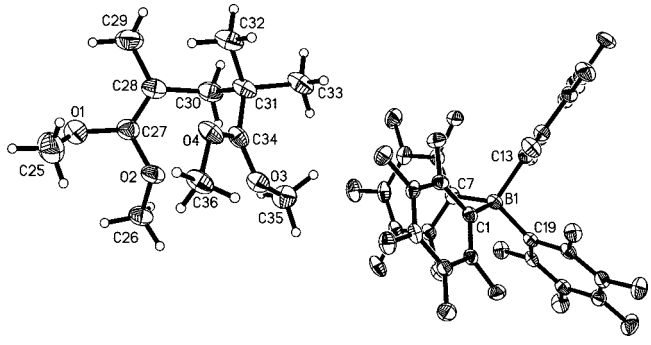

Figure 1. X-ray crystal structure of $[(MeO)_2C{=}CMeCH_2\text{-}CMe_2C(OMe)_2]^+[B(C_6F_5)_4]^-$ (**1**). Selected bond lengths [Å] and angels [deg]: O(1)−C(27) 1.366(3), O(2)−C(27) 1.381(2), O(3)−C(34) 1.278(2), O(4)−C(34) 1.274(2), C(27)−C(28) 1.325(3), C(31)−C(34) 1.514(3), B−C(1) 1.661(2), B−C(7) 1.658(3), B−C(13) 1.655(3), B−C(19) 1.655(3); O(1)−C(27)−O(2) 115.28(17), O(1)−C(27)−C(28) 124.1(2), O(2)−C(27)−C(28)120.66(19),O(3)−C(34)−O(4)115.54(17),O(3)−C(34)−C(31) 128.39(17), O(4)−C(34)−C(31) 115.99(17).

Scheme 4. Formation of O-Bound (Silyl Ketene Acetal) vs C-Bound (Isobutyrate) Products

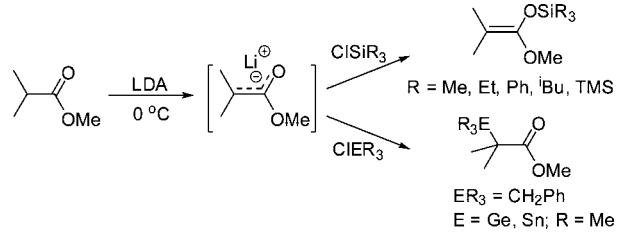

of analogous dimethylketene methyl benzyl, trimethylgermyl, and trimethylstannyl acetals: $Me_2C{=}C(OMe)OER_3$ (ER_3 = CH_2Ph; E = Ge, Sn, R = Me). However, this route led to the exclusive formation of the C-bound products (methyl isobutyrates) for group 14 elements other than silicon: $Me_2C(ER_3)\text{-}C(OMe){=}O$ (Scheme 4). These α-(ER_3)-substituted isobutyrates are *inactive* toward polymerization of (meth)acrylates upon activation with TTPB because they either do not react with TTPB at 25−80 °C (the benzyl derivative) or cannot be oxidatively activated by TTPB to give the desired active species (see Experimental Section).

Effect of Alkyl Group of Acetals: $Me_2C{=}C(OMe)OSiMe_3$ vs $Me_2C{=}C(O^iPr)OSiMe_3$. To systematically examine the SKA structural effects on polymerization characteristics, we first varied the alkyl group of acetals, followed by the silyl group (discussed in the next section). We reasoned that the sterics and electronics of the alkyl group of acetals may affect nucleophilicity of the SKA and stability or crystallizability of the resulting C−C bond coupling product in the activation (chain initiation) step upon treatment with TTPB.

The C−C bond coupling product (i.e., the active propagating species) obtained from oxidative activation of the isopropyl derivative $Me_2C{=}C(O^iPr)OSiMe_3$ with TTPB is also not crystallizable. Under the identical conditions, the MMA polymerization by $Me_2C{=}C(O^iPr)OSiMe_3$ in CH_2Cl_2 at 25 °C proceeds in the same, living fashion as that by the methyl derivative ^{Me}SKA, producing PMMA with the same syndiotacticity. The polymerization initiated by isopropyl trimethylsilyl acetal also follows zero-order kinetics in monomer concentration [M] (Figure 2), although the apparent rate of the polymerization by ^{Me}SKA is ∼1.2 times of that of the isopropyl trimethylsilyl acetal as shown by the slopes of two zero-order kinetic plots (Figure 2).

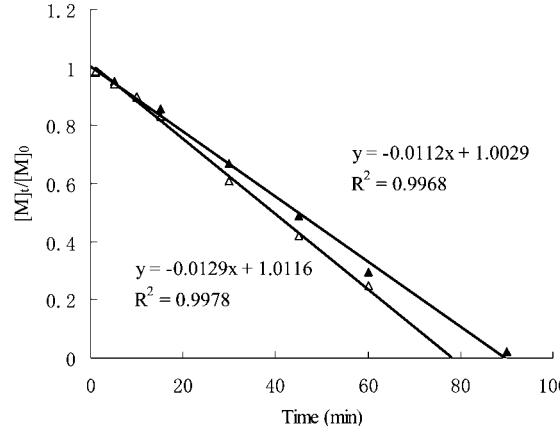

Figure 2. Zero-order plots of $[M]_t/[M]_0$ vs time for the methyl methacrylate (MMA) polymerization by the $Me_2C{=}C(O^iPr)OSiMe_3$ (▲) and $Me_2C{=}C(OMe)OSiMe_3$ (Δ) in CH_2Cl_2 (10 mL) at 25 °C in a MMA/SKA/TTPB ratio = 800/2/1: $[MMA]_0$ = 0.935 M, $[SKA]_0$ = 2.34 mM, $[TTPB]_0$ = 1.17 mM.

Table 1. Results of Methacrylate and Acrylate Polymerization by ^{iBu}SKA + 0.09 TTPB[a]

run no.	M (co-M)	solvent	time (min)	conv (%)	$10^{-4}M_n$[b] (g/mol)	PDI[b] (M_w/M_n)	I^*[c] (%)
1	*n*-BA	toluene	1	100	2.43	1.07	105
2	MMA	toluene	210	99	2.16	1.07	93
3	MMA	CH_2Cl_2	215	99	2.08	1.07	96
4	BMA	toluene	1320	100	4.91	1.08	58
5	BMA	CH_2Cl_2	780	100	4.21	1.07	67
6	MMA(*n*-BA)	toluene	$t_M + t_{co\text{-}M}$	100	4.53	1.13	101
7	MMA(*n*-BA)	CH_2Cl_2	$t_M + t_{co\text{-}M}$	100	4.48	1.09	102

[a] Carried out in 10 mL of solvent at room temperature (~25 °C) with monomer conversion being measured by NMR. The employed $[M]_0/[^{iBu}SKA]_0/[TTPB]_0$ ratio is 400/2.2/0.2, which corresponds to a [M]/[I] ratio of 200 or 400 for block copolymerization. [b] M_n and PDI determined by GPC relative to PMMA standards in $CHCl_3$. [c] Initiator efficiency (I^*) = M_n(calcd)/M_n(exptl), where M_n(calcd) = MW(M) × [M]/[I] × conversion % + MW (chain-end groups).

Effect of Silyl Group of Acetals $Me_2C{=}C(OMe)OSiR_3$ (R = Me, Et, Ph, ^{i}Bu, TMS). It is not unexpected that variations of the alkyl group of acetals did not show any appreciable effects on polymerization characteristics (vide supra) as only the chain initiation step would be impacted by the nature of the alkyl group. On the other hand, the silyl group of the acetal should have much more pronounced, direct effects on polymerization because the current polymerization is catalyzed by the *silyl cation* "R_3Si^+" derived from the SKA initiator upon activation with TTPB. To this end, we carried out comparative studies of (meth)acrylate polymerizations with five different SKA initiators varying R (Me, Et, Ph, ^{i}Bu, TMS) of the R_3Si group.

Under our standard polymerization screening conditions (i.e., $[MMA]_0/[SKA]_0/[TTPB]_0$ = 400/2/1, 25 °C, CH_2Cl_2), the polymerization by ^{Me}SKA achieved quantitative MMA conversion in <25 min. Replacing ^{Me}SKA with ^{Et}SKA, ^{Ph}SKA, ^{iBu}SKA, or ^{TMS}SKA resulted in considerably lower polymerization activity; for example, the MMA polymerizations by ^{iBu}SKA and ^{TMS}SKA are about 5 and 175 times slower than that by the parent ^{Me}SKA, respectively. On the other hand, the syndiotacticity of the resulting PMMA is noticeably enhanced by using larger alkylsilyl, arylsilyl, or silylsilyl groups: 73% *rr* by ^{Ph}SKA or ^{iBu}SKA and 77% *rr* by ^{TMS}SKA, compared to 70% *rr* by ^{Me}SKA.

Although ^{Me}SKA is the best initiator within this series for the polymerization of methacrylates (e.g., MMA, BMA) in terms of both polymerization activity and control, it is a poor initiator for acrylate (e.g., *n*-BA) polymerization, unable to achieve quantitative monomer conversion, even with extended reaction time (6 h) or at low temperature (0 °C), and affords P(*n*-BA) with broad MWDs. For example, with $[n\text{-BA}]_0/[^{Me}SKA]_0/[TTPB]_0$ = 400/2/1 (for a [M]/[I] ratio of 400) in CH_2Cl_2, the polymerization at 25 °C for 6 h achieved only 24.6% maximum conversion, indicative of substantial chain termination side reactions present in the acrylate polymerization by ^{Me}SKA; the final polymer has $M_n = 1.55 \times 10^4$ and PDI = 1.63. The polymerization at 0 °C is improved; monomer conversion at 1 h was 69.9%, the polymer M_n is 2.63×10^4, and PDI is 1.23. *Most remarkably,* switching from ^{Me}SKA to ^{iBu}SKA for acrylate polymerization under identical conditions resulted *extremely rapid and also living/controlled* polymerization at 25 °C, achieving 100% monomer conversion (by NMR) in <1 min of reaction time, reflecting a rate enhancement for *n*-BA polymerization of $>10^3$!

Prompted by this exciting finding, we examined acrylate and methacrylate polymerizations by ^{iBu}SKA under much more dilute catalyst conditions (i.e., 0.05 mol % TTPB relative to monomer) for a better control of reaction exothermicity. As can be seen from Table 1, with a $[n\text{-BA}]/[^{iBu}SKA]$ ratio of 200 at 25 °C, quantitative monomer conversion was achieved in 1 min, affording P(*n*-BA) of $M_n = 2.43 \times 10^4$ with a narrow MWD (PDI = 1.07), giving an essentially quantitative initiator efficiency (run 1). This acrylate polymerization is similarly highly effective and active in *aliphatic solvents* such as cyclohexane, producing P(*n*-BA) with PDI = 1.06.

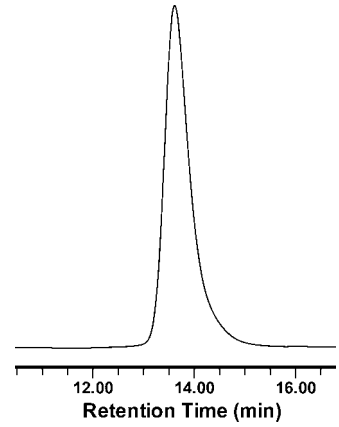

Figure 3. Representative GPC trace of diblock copolymer PMMA-*b*-P(*n*-BA) ($M_n = 4.48 \times 10^4$, PDI = 1.09) produced by the ^{iBu}SKA + 0.1 TTPB system in CH_2Cl_2 at 25 °C (run 7, Table 1).

In contrast, the polymerization of MMA by ^{iBu}SKA is sharply slower than that by ^{Me}SKA, although both initiators effect the living/controlled polymerization. Specifically, under identical conditions ($[MMA]_0/[SKA]_0/[TTPB]_0$ = 400/2.2/0.2, CH_2Cl_2, 25 °C), the polymerization by ^{Me}SKA achieved quantitative MMA conversion in 65 min ($M_n = 2.12 \times 10^4$, PDI = 1.08), whereas the polymerization by ^{iBu}SKA took 215 min to convert all of the monomer to the polymer ($M_n = 2.08 \times 10^4$, PDI = 1.07, run 3). Switching reaction solvent from CH_2Cl_2 to toluene had no noticeable impact on MMA polymerization characteristics (runs 2 vs 3) but a large effect on polymerization activity of the bulkier BMA monomer by ^{iBu}SKA; specifically, the BMA polymerization by ^{iBu}SKA becomes much slower, requiring 13 h (in CH_2Cl_2, run 5) or 23 h (in toluene, run 4) to achieve quantitative monomer conversions with significantly decreased initiator efficiencies (i.e., deflated M_n values). The above results reveal the importance of the SKA initiator−monomer structure matching: small silyl group initiators work best for methacrylates, while bulky silyl group initiators work best for less sterically hindered, active α-H bearing acrylate monomers.

Block copolymerization of MMA and *n*-BA in either toluene (run 6) or CH_2Cl_2 (run 7) at 25 °C produced well-defined block copolymer PMMA-*b*-P(*n*-BA) of $M_n = 4.53 \times 10^4$, PDI = 1.13 and $M_n = 4.48 \times 10^4$, PDI = 1.09 in toluene and in CH_2Cl_2 (Figure 3), respectively. The block copolymer M_n is a sum of two homopolymer's M_n with a unimodal MWD, and the block copolymerization in both solvents is highly effective, achieving quantitative initiator efficiencies (runs 6 and 7). Interestingly, this block copolymer cannot be obtained by starting *n*-BA polymerization followed by MMA polymerization, the procedure of which produced only P(*n*-BA) homopolymer. Accordingly, statistical copolymerization of a MMA and *n*-BA mixture yielded only P(*n*-BA) homopolymer. There are two plausible reasons for this behavior, considering the livingness of P(*n*-BA) chain toward further *n*-BA additions and the livingness of

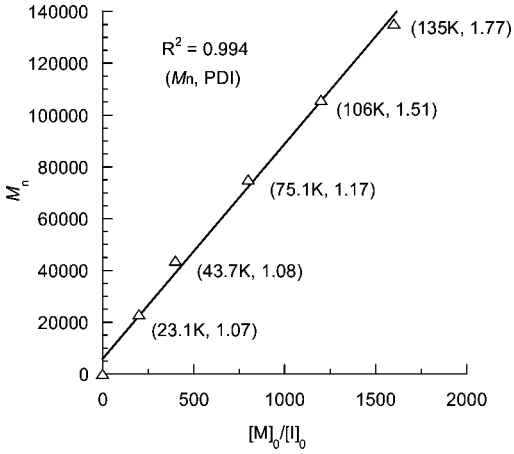

Figure 4. Plot of M_n of P(*n*-BA) vs $[M]_0/[I]_0$ ratios (10 mL toluene, 25 °C, 1 min). Amounts of *n*-BA (9.35 mmol) and TTPB (4.68×10^{-3} mmol) were fixed, whereas the amount of ^{iBu}SKA was varied to make the $[M]_0/[I]_0$ ratio = 200, 400, 800, 1200, and 1600. The M_n and PDI values for each $[M]_0/[I]_0$ ratio are included in parentheses.

PMMA chain toward further MMA or *n*-BA additions: (a) the *n*-BA-derived SKA chain end is not nucleophilic enough to attack MMA (incompatibility of nucleophilicity), or (b) the silyl cation capped by the penultimate *n*-BA unit cannot be transferred onto MMA (lack of monomer activation). More future work is needed to address this interesting issue.

The degree of control in the *n*-BA polymerization by ^{iBu}SKA was further examined with varied $[M]_0/[I]_0$ ratios = 200, 400, 800, 1200, and 1600. The polymerizations were carried out at 25 °C for 1 min, achieving 100% monomer conversions (by NMR) for all the ratios. A plot of the P(*n*-BA) M_n vs the $[M]_0/[I]_0$ ratio gave a linear relationship ($R^2 = 0.994$, Figure 4). The MWDs of the polymer remain narrow (≤1.17) for M_n up to 7.51×10^4 and then become broader with higher M_n polymer samples; this change is most likely a result of chain transfer processes present in the high $[M]_0/[I]_0$ ratio polymerization because there is a gradual increase in initiator efficiencies from a nearly quantitative value to ~150% as the $[M]_0/[I]_0$ ratio goes from 200 to 1600. It is noteworthy that the polymerization of *n*-BA by the bulkier ^{TMS}SKA is also highly effective, although its activity is somewhat lower than ^{iBu}SKA (e.g., with a $[M]_0/[I]_0$ ratio of 1600 in toluene at 25 °C, ^{TMS}SKA achieved 85% or 100% *n*-BA conversion in 1 or 5 min, compared to 100% *n*-BA conversion in 1 min using ^{iBu}SKA).

Effects of Activator (Counteranion). The current polymerization system is catalyzed by the in situ generated silyl cation "R_3Si^+" through oxidative activation of the SKA initiator by the trityl cation $[Ph_3C]^+$.[19] As the silyl cation chemistry is largely dictated by the coordinating nature of the counteranion,[35] we investigated the anion effects on characteristics of the MMA polymerization by employing four different trityl salts: $[Ph_3C][BF_4]$, $[Ph_3C][B(C_6F_5)_4]$, $[Ph_3C][(C_6F_5)_3Al{-}F{-}Al(C_6F_5)_3]$, and $[Ph_3C]$[*rac*-TRISPHAT]. The anion structures of these trityl salts are depicted in Scheme 5 to highlight their difference, especially in their anion size which should in part reflect on their ion-pairing strength.

Replacing TTPB with $[Ph_3C][BF_4]$ in the MMA polymerization initiated by ^{Me}SKA resulted in an inactive polymerization system. Inspection of the reaction of ^{Me}SKA with $[Ph_3C][BF_4]$ at room temperature by NMR showed the formation of the adduct $Ph_2C{=}C(CH{=}CH)_2CHCMe_2C(OMe){=}O$ (Scheme 6),[19,36] a result of *electrophilic addition* of $[Ph_3C]^+$, via the *para*-carbon of Ph, to ^{Me}SKA, rather than the formation of the desired active species structure by oxidative activation via vinylogous hydride abstraction of ^{Me}SKA with $[Ph_3C]^+$.[19] The coproduct

Scheme 5. Variations of Activator (and Thus Anion) Structures

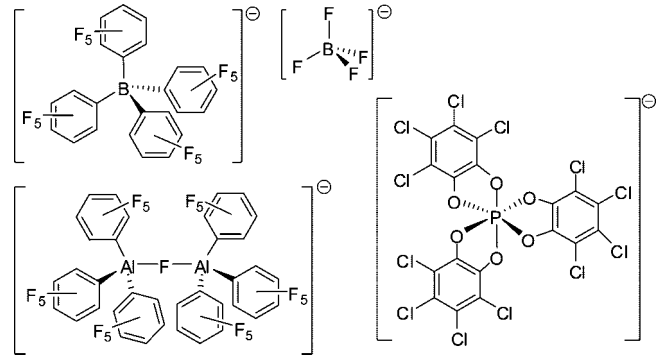

Scheme 6. Electrophilic Addition Reaction of ^{Me}SKA with $[Ph_3C][BF_4]$

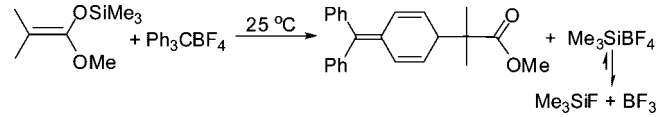

of this reaction, $[Me_3Si][BF_4]$, undergoes rapid ligand redistribution to give two neutral species Me_3SiF and BF_3 (see Experimental Section), thus quenching the generated silyl cation. The same electrophilic addition product was also observed from the reaction of ^{Me}SKA + $[Ph_3C][ClO_4]$ at 25 °C.[36]

MMA polymerization using a ^{Me}SKA and $[Ph_3C][(C_6F_5)_3Al{-}F{-}Al(C_6F_5)_3]$ combination in toluene yielded no polymer formation under various reaction conditions (extended reaction times up to 16 h and varied temperatures from 25 to −20 °C). Monitoring the direct reaction of these two reagents by NMR showed, in this case, that the oxidative activation via vinylogous hydride abstraction of ^{Me}SKA with $[Ph_3C]^+$ did occur, but the instability of the fluoride-bridged dialuminate anion quenched the generated silyl cation via again formation of Me_3SiF.

Lastly, the $[Ph_3C]^+$ cation paired with the racemic, hexacoordinate bulky chiral phosphate anion [*rac*-TRISPHAT]$^-$ was used to replace TTPB for the MMA polymerization initiated by^{Me}SKA in CH_2Cl_2 at 25 °C. The rate of the polymerization is approximately one-third of that observed for TTPB, although the syndiotacticity of the resulting PMMA produced by $[Ph_3C]$[*rac*-TRISPHAT] is slightly higher (73% *rr*) than that (70% *rr*) by TTPB. Apparently, when compared to the anion $[B(C_6F_5)_4]^-$, the bulky, chiral phosphate anion [*rac*-TRISPHAT]$^-$ actually reduced polymerization activity by 3-fold, presumably due to its stronger coordination to the silyl cation resulting from the chloride substituents on the phenyl rings, and only marginally altered the stereoselectivity of the current polymerization system under the present conditions.

Conclusions

In summary, the above structure−reactivity relationship studies of the recently developed polymerization system, which is effected by the highly active and bifunctional propagating species derived from oxidative activation of ketene silyl acetals with a catalytic amount of the activator TTPB, have revealed a few important features of this polymerization. First, there are no appreciable effects on polymerization observed for variations of the alkyl group of acetals. Second, among the group 14 (C, Si, Ge, and Sn)-based dimethylketene acetals investigated, only the silyl acetals can be oxidatively activated by TTPB to the desired active propagating species that promote highly efficient and active polymerization of (meth)acrylates. Third, there exhibits marked anion structure effects on polymerization

characteristics, reflecting on the relative anion stability and coordinating ability with respect to the highly reactive silyl cation. Among the four trityl salts investigated in this study, the active species paired with the $[B(C_6F_5)_4]^-$ anion gives the highest polymerization activity and degree of polymerization control.

Lastly and *most significantly*, there is remarkable selectivity of the silyl group structure of the acetal initiator (and thus the silyl cation catalyst structure) for monomer structure. Initiators having small silyl groups such as ^{Me}SKA effect highly active and efficient polymerization of methacrylates, but they are poor initiators for polymerization of less sterically hindered, active α-H bearing acrylate monomers. On the other hand, initiators incorporating bulky silyl groups such as ^{iBu}SKA initiators exhibit low activity toward methacrylate polymerization but *exceptionally high activity and degree of control* for acrylate polymerization 25 °C in polar noncoordinating (CH_2Cl_2), aromatic (toluene), or aliphatic (cyclohexane) solvents. Thus, *n*-BA polymerization by ^{iBu}SKA in combination with a catalytic amount of TTPB (0.05 mol % relative to monomer) is complete within 1 min, producing P(*n*-BA) with narrow MWDs (PDI = 1.07−1.17) for M_n up to 7.51×10^4 or higher M_n ($>10^5$) at the expense of broader MWDs. The polyacrylate M_n is controlled by the $[M]_0/[I]_0$ ratio employed, and the polymerization exhibits typically a quantitative initiator efficiency with low to moderately high $[M]_0/[I]_0$ ratios employed. Well-defined methacrylate−acrylate block copolymer PMMA-*b*-P(*n*-BA) (PDI = 1.09) can thus be realized using this system at ambient temperature.

Acknowledgment. This work was supported by the donors of the Petroleum Research Fund, administered by the American Chemical Society. We thank Susie Miller for the single-crystal X-ray diffraction analysis and Boulder Scientific Co. for the gift of $B(C_6F_5)_3$ and $[Ph_3C][B(C_6F_5)_4]$.

Supporting Information Available: Crystallographic data for **1**. This material is available free of charge via the Internet at http://pubs.acs.org.

References and Notes

(1) Hsieh, H. L.; Quirk, R. P. *Anionic Polymerization. Principles and Practical Applications*; Marcel Dekker: New York, 1996.
(2) Rodriguez-Delgado, A.; Chen, E. Y.-X. *J. Am. Chem. Soc.* **2005**, *127*, 961–974.
(3) For comprehensive reviews, see:(a) Baskaran, D.; Müller, A. H. E. *Prog. Polym. Sci.* **2007**, *32*, 173–219. (b) Baskaran, D. *Prog. Polym. Sci.* **2003**, *28*, 521–581. (c) Vlček, P.; Lochmann, L. *Prog. Polym. Sci.* **1999**, *24*, 793–973. (d) Zune, C.; Jérôme, R. *Prog. Polym. Sci.* **1999**, *24*, 631–664. (e) Hatada, K.; Kitayama, T.; Ute, K. *Prog. Polym. Sci.* **1988**, *13*, 189–276. (f) Van Beylen, M.; Bywater, S.; Smets, G.; Szwarc, M.; Worsfold, D. J. *Adv. Polym. Sci.* **1988**, *86*, 87–143.
(4) Webster, O. W.; Hertler, W. R.; Sogah, D. Y.; Farnham, W. B.; RajanBabu, T. V. *J. Am. Chem. Soc.* **1983**, *105*, 5706–5708.
(5) Webster, O. W. *Adv. Polym. Sci.* **2004**, *167*, 1–34.
(6) (a) Müller, A. H. E.; Litvinenko, G.; Yan, D. *Macromolecules* **1996**, *29*, 2346–2353. (b) Quirk, R. P.; Kim, J.-S. *J. Phys. Org. Chem.* **1995**, *8*, 242–248. (c) Quirk, R. P.; Bidinger, G. P. *Polym. Bull.* **1989**, *22*, 63–70.
(7) Sogah, D. Y.; Hertler, W. R.; Webster, O. W.; Cohen, G. M. *Macromolecules* **1987**, *20*, 1473–1488.
(8) Hertler, W. R.; Sogah, D. Y.; Webster, O. W.; Trost, B. M. *Macromolecules* **1984**, *17*, 1415–1417.
(9) Jung, M. E.; Pan, Y.-G.; Rathke, M. W.; Sullivan, D. F.; Woodbury, R. P. *J. Org. Chem.* **1977**, *42*, 3961–3963.
(10) (a) Bochmann, M.; Lancaster, S. J. *J. Organomet. Chem.* **1992**, *434*, C1–C5. (b) Chien, J. C. W.; Tsai, W.-M.; Rausch, M. D. *J. Am. Chem. Soc.* **1991**, *113*, 8570–8571.
(11) Lian, B.; Toupet, L.; Carpentier, J.-F. *Chem.—Eur. J.* **2004**, *10*, 4301–4307.
(12) Ning, Y.; Chen, E. Y.-X. *J. Am. Chem. Soc.* **2008**, *130*, 2463–2465.
(13) Chen, E. Y.-X.; Marks, T. J. *Chem. Rev.* **2000**, *100*, 1391–1434.
(14) Lambert, J. B.; Zhang, S.; Stern, C. L.; Huffman, J. C. *Science* **1993**, *260*, 1917–1918.
(15) (a) Kobayashi, S.; Murakami, M.; Mukaiyama, T. *Chem. Lett.* **1985**, *14*, 1535–1538. (b) Kobayashi, S.; Murakami, M.; Mukaiyama, T. *Chem. Lett.* **1985**, *14*, 953–956. (c) Mukaiyama, T.; Kobayashi, S.; Murakami, M. *Chem. Lett.* **1985**, *14*, 447–450. (d) Mukaiyama, T.; Kobayashi, S.; Murakami, M. *Chem. Lett.* **1984**, *13*, 1759–1762.
(16) (a) Noyori, R.; Murata, S.; Suzuki, M. *Tetrahedron* **1981**, *37*, 3899–3910. (b) Murata, S.; Suzuki, M.; Noyori, R. *J. Am. Chem. Soc.* **1980**, *102*, 3248–3249.
(17) Oishi, M.; Aratake, S.; Yamamoto, H. *J. Am. Chem. Soc.* **1998**, *120*, 8271–8272.
(18) Ute, K.; Ohnuma, H.; Kitayama, T. *Polym. J.* **2000**, *32*, 1060–1062.
(19) Zhang, Y.; Chen, E. Y.-X. *Macromolecules* **2008**, *41*, 36–42.
(20) Bolig, A. D.; Chen, E. Y.-X. *J. Am. Chem. Soc.* **2001**, *123*, 7943–7944.
(21) (a) Stojcevic, G.; Kim, H.; Taylor, N. J.; Marder, T. B.; Collins, S. *Angew. Chem., Int. Ed.* **2004**, *43*, 5523–5526. (b) Li, Y.; Ward, D. G.; Reddy, S. S.; Collins, S. *Macromolecules* **1997**, *30*, 1875–1883.
(22) Allen, R. D.; Long, T. E.; McGrath, J. E. *Polym. Bull.* **1986**, *15*, 127–134.
(23) Feng, S.; Roof, G. R.; Chen, E. Y.-X. *Organometallics* **2002**, *21*, 832–839.
(24) (a) Lee, C. H.; Lee, S. J.; Park, J. W.; Kim, K. H.; Lee, B. Y.; Oh, J. S. *J. Mol. Catal., A: Chem.* **1998**, *132*, 231–239. (b) Biagini, P.; Lugli, G.; Abis, L.; Andreussi, P. U.S. Pat. 5,602269, **1997**.
(25) (a) Mcelvain, S. M.; Venerable, J. T. *J. Am. Chem. Soc.* **1950**, *72*, 1661–1669. (b) Mcelvain, S. M.; Davie, W. R. *J. Am. Chem. Soc.* **1951**, *73*, 1400–1402.
(26) Hatano, M.; Takagi, E.; Ishihara, K. *Org. Lett.* **2007**, *9*, 4527–4530.
(27) Chen, M.-C.; Roberts, J. A. S.; Marks, T. J. *Organometallics* **2004**, *23*, 932–935.
(28) (a) Favarger, F.; Ginglinger, C. G.; Monchaud, D.; Lacour, J. *J. Org. Chem.* **2004**, *69*, 8521–8524. (b) Lee, H. S.; Novak, B. *Polym. Prepr.* **2005**, *46*, 839–840.
(29) Földes, R. S.; Kollár, L.; Heil, B. *J. Organomet. Chem.* **1991**, *408*, 297–304.
(30) (a) Oisaki, K.; Suto, Y.; Kanai, M.; Shibasaki, M. *J. Am. Chem. Soc.* **2003**, *125*, 5644–5645. (b) Ainsworth, C.; Chen, F.; Kuo, Y.-N. *J. Organomet. Chem.* **1972**, *46*, 59–71.
(31) Arnold, R. T.; Kulenoviæ, S. T. *J. Org. Chem.* **1980**, *45*, 891–894.
(32) Rodriguez-Delgado, A.; Chen, E. Y.-X. *Macromolecules* **2005**, *38*, 2587–2594.
(33) (a) Bovey, F. A.; Mirau, P. A. *NMR of Polymers*; Academic Press: San Diego, CA, 1996. (b) Chujo, R.; Hatada, K.; Kitamaru, R.; Kitayama, T.; Sato, H.; Tanaka, Y. *Polym. J.* **1987**, *19*, 413–424. (c) Ferguson, R. C.; Ovenall, D. W. *Polym. Prepr.* **1985**, *26*, 182–183. (d) Subramanian, R.; Allen, R. D.; McGrath, J. E.; Ward, T. C. *Polym. Prepr.* **1985**, *26*, 238–240.
(34) SHELXTL, Version 6.12; Bruker Analytical X-ray Solutions, Madison, WI, **2001**.
(35) For recent examples, see: (a) Zhang, Y.; Huynh, K.; Manners, I.; Reed, C. A. *Chem. Commun.* **2008**, 494–496. (b) Küppers, T.; Bernhardt, E.; Eujen, R.; Willner, H.; Lehmann, C. W. *Angew. Chem., Int. Ed.* **2007**, *46*, 6346–6349. (c) Kim, K.-C.; Reed, C. A.; Elliott, D. W.; Mueller, L. J.; Tham, F.; Lin, L.; Lambert, J. B. *Science* **2002**, *297*, 825–827.
(36) Fukuzumi, S.; Ohkubo, K.; Otera, J. *J. Org. Chem.* **2001**, *66*, 1450–1454.

MA801125Y